Gas Absorption in a Wetted-Wire Column

Hirofumi Migita, Kohei Soga, and Yasuhiko H. Mori
Dept. of Mechanical Engineering, Keio University, Yokohama 223-8522, Japan

DOI 10.1002/aic.10483
Published online May 23, 2005 in Wiley InterScience (www.interscience.wiley.com).

This study aims to examine the performance, as a gas absorber, of a "wetted-wire column," a novel gas–liquid contact device equipped with a bundle of built-in vertically oriented wires. This device allows a liquid absorbent to flow down each wire, being in contact with a gas mixture flowing countercurrently. A prototype column having 109 wires was constructed and then tested in experimental CO_2-absorption operations, using aqueous monoethanolamine absorbents. In every operation, a monoethanolamine solution was supplied to the column at a constant rate such that its flow on each wire assumed a "string-of-beads" pattern consisting of annular thin liquid films sheathing the wire and teardrop-shaped liquid beads alternately aligned on the wire at regular intervals. It was confirmed that the wetted-wire column has an absorption performance quite comparable to conventional packed-bed columns, while it imposes, on the internal gas flow, only a pressure loss smaller than that in packed-bed columns of the same height by one to two orders. © 2005 American Institute of Chemical Engineers *AIChE J,* 51: 2190–2198, 2005
Keywords: gas absorption; gas–liquid contactor, CO_2 separation; mass transfer; mass-transfer equipment

Introduction

Gas absorption using liquid absorbents is one of the common mass-transfer operations widely used in industry for separating some components (such as useful, toxic, or environmentally unfavorable species) from gas mixtures before feeding them to subsequent in-plant operations or releasing them to the atmosphere. Separating carbon dioxide (CO_2) from the flue gases in fossil-fuel–fired power plants is a potential application of such a gas-absorption operation, which is to mitigate global warming attributed to the so-called greenhouse effect. To minimize the additional energy consumption indispensable for treating a huge amount of low-pressure (not much higher than atmospheric pressure) gases of no further use, it is crucially important to devise gas–liquid contactors that allow effective gas absorption without prepressurizing the gases to balance the hydrodynamic pressure losses inside the contactors.

In general, the requirement for high gas-absorption performance (such as high transfer efficiency or high volumetric mass transfer coefficient) and that for low gas-side pressure loss conflict with each other. For example, packed-bed columns have much higher gas-absorption performance than that of wetted-wall columns and spray columns when compared at fixed gas- and liquid-flow rates, but force the gas phase to undergo much larger pressure losses than wetted-wall and spray columns. A large gas–liquid contact area per unit volume and good mixing in the liquid absorbent while flowing over geometrically complicated packings inside each packed-bed column are major factors that provide a high volumetric mass-transfer coefficient in the column. Further, a relatively long residence time of the liquid absorbent inside the column should contribute to increasing the liquid-side transfer efficiency. On the other hand, a large form drag imposed on the gas flow as a consequence of the geometry of the packings causes a large gas-side pressure loss inside the packed-bed column. Thus, it is desirable to devise such a type of gas–liquid contactor that keeps the advantages of packed-bed columns—that is, the long residence time of, and sufficient mixing inside, the liquid absorbent in which the major resistance to mass transfer lies—and gives a much smoother gas-flow pass than that of packed-bed columns.

Current address of H. Migita: Hitachi Construction Machinery Co., Ltd., 650 Kandatsu-cho, Tsuchiura-shi, Ibaraki-ken 300-0013, Japan.
Correspondence concerning this article should be addressed to Y. H. Mori at yhmori@mech.keio.ac.jp.

We expect that, as already suggested in our previous studies,[1,2] *wetted-wire columns* will possibly satisfy the requirements described above, where *wetted-wire columns* refer to vertical columns each equipped with internal multiple wires vertically hung such that a liquid absorbent flows down the wires while contacting a countercurrent gas flow. Desirably, the liquid absorbent flows down each wire in the form of a *string of beads*, that is, a distinct on-wire liquid-flow pattern consisting of annular thin films sheathing a wire and teardrop-shaped liquid beads alternately aligned on the wire at regular intervals, so that continuous bead-to-film and film-to-bead mass displacement occurs as a result of the difference between the fall velocity of the beads and the flow velocity of the films, thereby strengthening the internal mixing of the absorbent on the wire. Although we have already studied both experimentally and theoretically the physical and chemical absorption of CO_2 from an upward-flowing CO_2/N_2 mixture into liquid water and an aqueous monoethanolamine (MEA) solution, respectively, each flowing downward in the *string-of-beads* pattern on a single wire vertically hung in the gas flow,[1,2] we have not yet demonstrated any multiple-wire column actually usable for gas absorption. Therefore, the estimated advantage of wetted-wire columns over conventional gas–liquid contact devices is yet to be confirmed.

In the present study, we constructed a prototype wetted-wire column equipped with 109 regularly aligned wires and tested its gas-absorption performance as well as the gas-side pressure loss characteristics. As detailed below, we have confirmed that the gas-absorption performance of the wetted-wire column is comparable, or even superior, to that of a typical packed-bed column having the same height of gas–liquid contact section and that the gas-side pressure loss in the former is far smaller than that in the latter.

Constructing a Prototype Wetted-Wire Column

Although we have demonstrated the potential advantage of wetted-wire columns over conventional gas–liquid contactors based on our single-wire experiments,[1,2] we still need to solve a technical problem—to put the idea of wetted-wire columns into practice—of how to distribute the liquid absorbent onto all wires in each column. Note that the number of wires to be installed in each wetted-wire column may be as large as several hundreds or even larger; the number of wires in a column whose diameter is about 1 m may exceed 10,000. We need to have a device for evenly distributing the absorbent onto these wires. The device should preferably be simple so that it does not substantially increase the cost of column construction. After some trial-and-error tests, we contrived an effectual device—an absorbent reservoir with its bottom plate equipped with regularly aligned cylindrical nozzles through each of which a top portion of a wire was inserted into the reservoir. This device was applied to the prototype wetted-wire column, which is outlined below.

Figure 1 illustrates the structure of the prototype wetted-wire column that we constructed to confirm the practicability of the idea of wetted-wire columns and for use in the gas-absorption experiments described later. The major portion of the column is confined in two, vertically oriented, transparent poly(methyl methacrylate) (PMMA) pipes (70 mm ID), one being placed on the top of the other. Except for a short section at its bottom end,

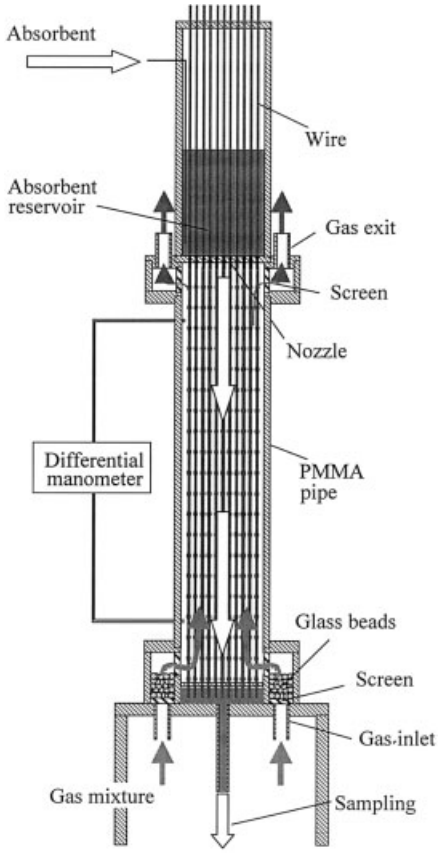

Figure 1. Prototype wetted-wire column equipped with 109 wires.

the space inside the lower pipe is used for the contact of a gas mixture flowing upward with a liquid absorbent flowing down the wires, whereas the space inside the upper pipe is used as a reservoir for the absorbent. The bottom of the upper pipe is closed by a PMMA plate on which 109 holes are drilled. A stainless-steel tube, 1.12 (+0.04/−0.02) mm ID and 10 mm long, which is to serve as a nozzle, is fitted into each hole so tightly that the absorbent never leaks from the reservoir into the lower space through a gap between the outer surface of the tube and the bottom plate. Inserted into the above tube (that is, one of 109 nozzles) is a "wire"—actually a straight stainless-steel tube, 0.88 ± 0.02 mm OD—that extends to the entire height of the column. The geometrical arrangement of the 109 wires over the cross section of the column is illustrated in Figure 2; the wires are so aligned at intervals of 6 mm as to be located at the apices of equilateral triangles. Figure 3 shows the nozzle/wire assembly thus constructed. The lower end of each wire is inserted into a hole drilled through a PMMA plate that separates the gas–liquid contact section (300 or 675 mm in height) above it from the absorbent-collecting section (~20 mm in height) below it.

The absorbent continuously poured into the reservoir at a constant rate forms a pool of a constant depth and thereby steadily flows onto each of the 109 wires in the lower gas–liquid contact section through the annular space between the wire and the nozzle. The driving force for this absorbent flow is the hydrostatic head sustained in the reservoir, which is only of the order of 1 kPa or less. The absorbent having flowed

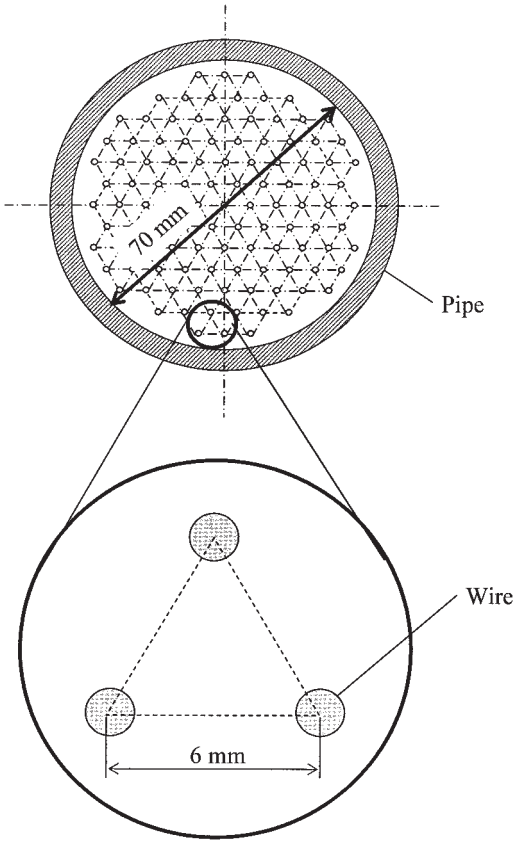

Figure 2. Arrangement of 109 wires inside the wetted-wire column.

The wire diameter is 0.88 mm.

down the wires spills on the wire-holding plate and falls into the absorbent-collecting section below it through 106 drain holes, each 2.5 mm in diameter, drilled on the plate. Inside this section, the absorbent forms a shallow pool on the bottom plate of the entire column and is continuously drained out of the column through a stainless-steel tubing connected to the central opening of the bottom plate. Occasionally, the absorbent thus drained is sampled for measuring the amount of CO_2 absorbed in it.

The gas–liquid contact section is equipped with gas inlet and outlet assemblies at its bottom and top, respectively. The gas inlet is a peripheral opening enveloped in an annular chamber. Glass beads, 5.0 ± 0.5 mm in diameter, are packed in the lower half of the chamber to make the gas mixture flow through the bed of these beads and thereby have a circumferentially uniform velocity before it radially flows into the gas–liquid contact section. The gas-outlet assembly has a geometry similar to that of the inlet assembly, although no bed of glass beads is held inside. The gas mixture should radially flow into an annular chamber enveloping the exit, then flows out of the column through eight exhaust tubes circumferentially distributed over the ceiling of the chamber. These exhaust tubes extend only a few meters before they open to the exterior air so that the pressure in the gas–liquid contact section of the test column deviates little from atmospheric pressure, 0.101 MPa.

To determine the axial pressure drop in the gas mixture flowing upward in the gas–liquid contact section, four pressure-measuring ports are vertically aligned on the wall of the PMMA pipe that holds the gas–liquid contact section inside. Two of these ports may be connected, whereas the other two are blanked, to an electronic differential manometer (Manoace Model 130, Sayama Trading Co.) to measure the difference in static pressure between the two ports to an accuracy of 0.1 Pa.

Auxiliary devices connected to the wetted-wire column are a Kofloc PMG-1 gas blender, through which CO_2 and N_2 gases supplied from separate cylinders are blended in a prescribed proportion to form a gas mixture to be supplied to the bottom gas inlet of the column, and a nonpulsating double-plunger pump (Nippon Seimitsu Model NP-KX-700) to pump a liquid absorbent (an aqueous MEA solution) to the reservoir at the top of the column.

Description of Experiments

The prototype wetted-wire column described above (referred to as the "test column" hereafter) was used in the experiments of CO_2 absorption from a CO_2/N_2 mixture by an MEA solution and in the measurements of axial gas-side pressure drop. The outlines of these experimental operations and the processing of experimental data obtained are described in this section.

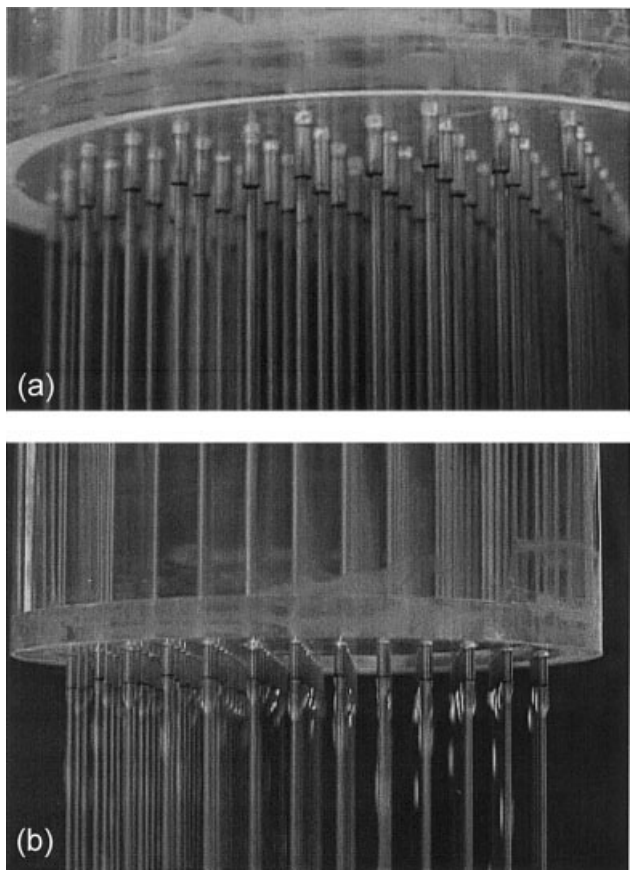

Figure 3. Nozzle/wire assembly at the top portion of the gas–liquid contact section.

(a) Upward view of the assembly; (b) nearly horizontal view of the assembly releasing an MEA solution onto wires. The PMMA pipe enclosing the gas–liquid contact section is removed for convenience in photography.

Table 1. Physical and Chemical Properties of CO_2/N_2 Gas Mixture (0.1 mole fraction of CO_2), Aqueous MEA Solutions, and CO_2–MEA Solution Systems at a Temperature of 25°C, a Total Pressure of 101.3 kPa, and a CO_2 Partial Pressure of 10.13 kPa

Property	CO_2/N_2	MEA Solution	
		15%	30%
Mass density, ρ_G, ρ_L (kg/m^3)	1.21[a]	1003[b]	1010[b]
Viscosity, μ_G, μ_L (mPa s)	1.73×10^{-2} [c]	1.45[d]	2.41[d]
Surface tension, σ_L (mN/m)		64.1[e]	60.1[e]
Overall solubility of CO_2			
c_{sat} (kg/m^3)		64.9[f]	127.6[g]
$\tilde{c}_{sat}$ (kmol/m^3)		1.47[f]	2.90[g]
Physical solubility of CO_2			
c_s (kg/m^3)		0.119[h]	
$\tilde{c}_s$ (kmol/m^3)		2.70×10^{-3} [h]	
Henry's constant, H [mol CO_2/(m^3 Pa)]		0.316×10^{-3} [h]	
Diffusivity of CO_2, D_G, D_L (m^2/s)	1.67×10^{-5} [i]	1.48×10^{-9} [j]	
Diffusivity of MEA, D_{AL} (m^2/s)		8.43×10^{-10} [k]	
CO_2–MEA reaction rate constant, k_r [m^3/(mol–MEA s)]		5.92[l]	

[a]Calculated by assuming the CO_2/N_2 mixture to be an ideal-gas mixture.
[b]Calculated by an empirical correlation given by Song et al.[3]
[c]Calculated on the basis of the Chapman–Enskog kinetic theory extended to low-pressure gas mixtures, using Eqs. 9-3.9, 9-4.3, and 9-5.4 given in the book of Reid et al.[4]
[d]Estimated by curve fitting to, or by extrapolating the curve fitted to, the experimental data of Hikita et al.[5]
[e]Calculated by an empirical correlation given by Vázquez et al.[6]
[f]Estimated by curve fitting to the experimental data of Lee et al.[7] and of Muhlbauer and Monaghan.[8]
[g]Estimated by curve fitting to the experimental data of Jou et al.[9]
[h]Estimated by using the N_2O analogy[10] to combine three empirical correlations given by Versteeg et al.,[11] one for the solubility of N_2O in MEA solutions and the other two for Henry's constants for CO_2–water and N_2O–water systems, respectively.
[i]Cited from Table 11-2 in the book of Reid et al.[4]
[j]Estimated using the N_2O analogy[12] to combine the value of N_2O–MEA solution diffusivity read by curve fitting to the experimental data of Sada et al.[13] with empirical correlations for CO_2–water and N_2O–water diffusivities, respectively, both given by Versteeg et al.[11]
[k]Calculated by the Wilke–Chang equation[14] incorporating an association-parameter value recommended by Hayduk and Laudie.[15]
[l]Calculated by empirical correlation given by Hikita et al.[16]

Experiments of CO_2 absorption

The procedure of the CO_2-absorption experiments generally followed that of our previous single-wire study.[2] A CO_2/N_2 mixture adjusted to 0.1 mole fraction of CO_2 by the gas blender was supplied to the test column at a constant rate. The liquid absorbent supplied to the test column to make contact with the gas mixture was 15 or 30 wt % MEA solution prepared from a reagent-grade sample of MEA (98.5 wt % certified purity) and deionized–distilled water. Some physical properties of the CO_2/N_2 mixture and the MEA solutions as well as the CO_2 solubility in the solutions are indicated in Table 1. The height of the gas–liquid contact section in the test column was adjusted to 300 mm. The flow rates of the gas mixture and the liquid absorbent were varied as operational parameters such that the superficial velocity of the gas mixture (ν_G) and that of the liquid absorbent (ν_L) fell in the range of 0.065–0.217 m/s and 0.30–1.26 mm/s, respectively. In each experiment, the absorbent draining out of the test column was sampled and analyzed by the precipitation–titration method[9] to quantify the amount of CO_2 absorbed per unit volume of the absorbent. All of the experimental operations were performed in a temperature-controlled laboratory at 25 ± 1°C.

Measurements of pressure drop in gas flow

The height of the gas–liquid contact section in the test column was elongated to 675 mm and the pressure drop over the axial length of 510 mm was measured, changing ν_G stepwise while holding ν_L constant at each of several different levels. A 15 wt % MEA solution was used exclusively as the liquid absorbent. For experimental convenience, this MEA solution in a fixed amount was being circulated by the double-plunger pump through the test column and an external flow-back tubing throughout the measurements. To prevent the solution from suffering any property change arising from CO_2 absorption, pure N_2 gas was used as the substitute for the CO_2/N_2 mixture throughout the measurements.

Data processing

The data obtained in the CO_2-absorption experiments were processed using either of two indices for evaluating the effectiveness of the gas-to-liquid CO_2 transfer: the liquid-side absorption efficiency E and the gas-based overall capacity coefficient (or volumetric mass-transfer coefficient) K_Ga. The absorption efficiency E is defined as

$$E = \frac{c_B - c_T}{c_{sat} - c_T} \tag{1}$$

where c denotes the mass of CO_2 absorbed into a unit volume of the liquid absorbent; subscripts T and B, respectively, stand for the top and the bottom of the test column and thereby indicate the liquid absorbent sampled before and after flowing down the wires in the test column; and "sat" denotes the saturation of the absorbent with CO_2 under the partial pressure of CO_2 adjusted to one-tenth of 1 atm (101.3 kPa). The values of c_{sat}, the solubility of CO_2 in the absorbent with respect to 15 and 30 wt % MEA solutions, are given in Table 1.

The overall capacity coefficient K_Ga is the product of K_G, the overall mass-transfer coefficient based on the gas–liquid inter-

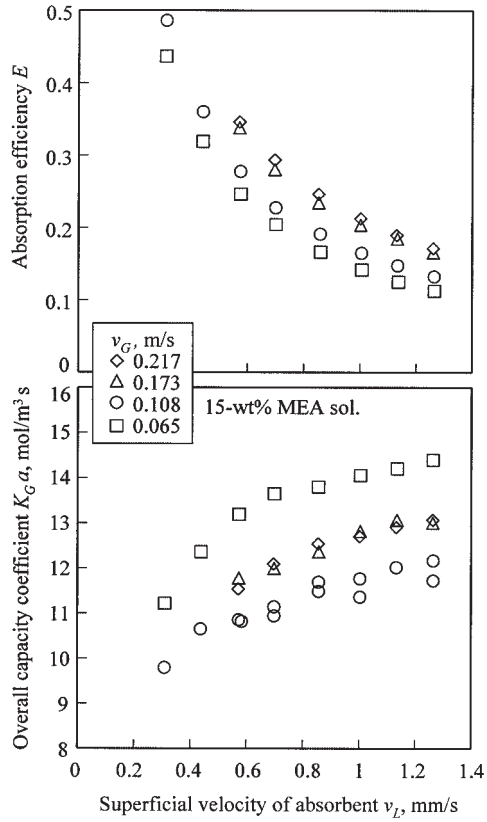

Figure 4. Absorption efficiency and gas-based overall capacity coefficient obtained with 15 wt % MEA solution applied to the prototype wetted-wire column.

facial area and on the gas-based expression for the CO_2 mole-fraction difference between the gas and liquid phases (thereby given in the unit of mol m^{-2} s^{-1}), and a, the gas–liquid interfacial area per unit volume in the test column. Following the formulation for CO_2 mass conservation given in Appendix A, we can write the above coefficient as follows

$$K_G a = \frac{\tilde{m}_n}{Z}\left[Y_B - Y_T + \ln\left(\frac{Y_B}{Y_T}\right)\right] \tag{2}$$

where $\tilde{m}_n$ is the superficial molar flux of the inert species (N_2 in the present experiments) across a horizontal cross section of the test column, Z is the height of the effective gas–liquid contact section in the test column (300 mm), and Y is the mixed-mean CO_2-to-N_2 molar ratio at each cross section of the column. The values of Y_T and Y_B are readily deduced from c_B and c_T, respectively.

Results and Discussion

Figure 4 demonstrates the CO_2-absorption performance exhibited by the test column when the 15 wt % MEA solution was used as the absorbent. The relevant experimental data are arranged in the form of the absorption efficiency E or the overall capacity coefficient $K_G a$ and plotted against v_L, the superficial velocity of the absorbent (that is, the volume flow rate of the absorbent divided by the cross-sectional area of the test column), for each level of v_G, the superficial velocity of the gas mixture (that is, the column-inlet volume flow rate of the CO_2/N_2 gas mixture divided by the cross-sectional area of the test column). We can readily recognize that E and $K_G a$ show opposite v_L dependencies: that is, an increase in v_L causes an increase in $K_G a$ but a decrease in E. These tendencies may be a consequence of the nature of the *string-of-beads* flow of the liquid absorbent on each wire. As revealed in the previous single-wire experiments,[1,2] an increase in the liquid flow rate on each wire causes simultaneous increases in the size and fall velocity of individual beads regularly aligned on the wire over a relatively low flow-rate range or, in a higher flow-rate range, a shortening of the linear intervals of the beads on the wire. Any of these changes in the *string-of-beads* flow resulting from an increase in the liquid flow rate should increase the gas–liquid interfacial area and enhance the mixing in both the liquid phase and the near-interface region in the gas phase, thereby enhancing the gas-to-liquid CO_2 transfer and giving higher $K_G a$ values. However, this effect is not sufficient to balance a linear increase in the absorption capacity with an increasing v_L, thus resulting in a decrease in E.

An increase in v_G causes a consistent increase in E. In contrast, the effect of v_G on $K_G a$ is not necessarily clear in Figure 4; the effect seems to be relatively weak. An increase in v_G should contribute to reducing the axial drop of the CO_2 concentration in the gas flow and to increasing the gas-side mass transfer coefficient. Both of these outcomes of increasing v_G could in principle affect E, whereas only the latter should affect $K_G a$. Our observation of only indefinite v_G dependency of $K_G a$ indicates that the major resistance to gas-to-liquid CO_2 transfer lies in the liquid phase and thus an increase in the gas-side mass transfer coefficient has little effect on the overall transfer coefficient. Consequently, it may be said that the observed increase in E with an increasing v_G is primarily explained by the resultant increase in the driving force for CO_2 transfer throughout the gas–liquid contact section instead of the possible increase in the mass transfer coefficient.

Figure 5 compares $K_G a$ vs. v_G relations obtained by use of

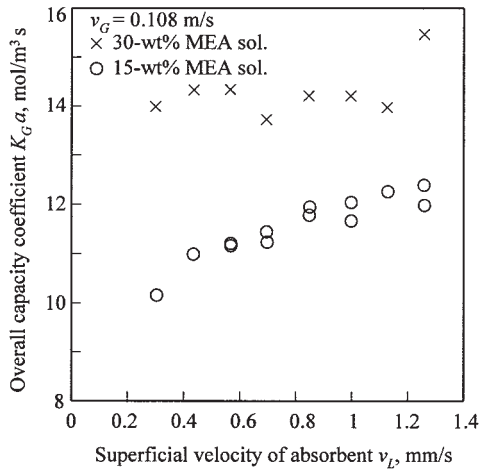

Figure 5. Variation in gas-based overall capacity coefficient depending on the MEA concentration in liquid absorbent supplied to the wetted-wire column.

the 15 and 30 wt % MEA solutions. The v_L dependency of K_Ga is weaker with the 30 wt % solution than that with the 15 wt % solution, and the excess of the former solution over the latter in K_Ga is reduced with an increase in v_L. The relative increase in K_Ga as the result of doubling the MEA concentration could never be twice as much but is only 17 to 40% over the *string-of-beads* flow regime. It is interesting to note that the above increase in K_Ga is still larger than that obtained by doubling the flow rate v_L of the 15 wt % MEA solution (see Figure 4) despite the same rate of MEA supply being required in doubling the MEA concentration and in doubling v_L. Such an advantage of increasing the MEA concentration over increasing v_L is presumably attributable, at least in part, to an increase in liquid viscosity with an increase in MEA concentration, which results in the formation of a train of beads aligned at shorter intervals and falling more slowly on each wire,[2] maintaining a larger gas–liquid interfacial area. An increase in the CO_2–MEA reaction rate constant with an increase in MEA concentration may also be another factor contributing to increasing K_Ga with an increasing MEA concentration.

It may be worth pointing out that the dependencies of E and K_Ga on v_L and MEA concentration in the absorbent demonstrated above are in qualitative agreement with the results of single-wire experiments of Uchiyama et al.[2] In comparing the results of both studies, one should note that the K_Ga vs. v_L relations observed in the present study generally correspond to the $\dot{M}$ vs. $\dot{V}_L$ relations obtained in the study of Uchiyama et al.,[2] where $\dot{V}_L$ and $\dot{M}$ denote the volume flow rate of an absorbent (15 or 30 wt % MEA solution) supplied onto each single wire and the rate of CO_2 absorption by the absorbent flowing down the wire, respectively.

To appraise the absorption performance demonstrated above, we compare it with the performance displayed by a conventional packed-bed column operated under the same conditions of gas and liquid-absorbent feeding. The packed-bed column is assumed to be packed with 1/2- or 1/4-in. ceramic

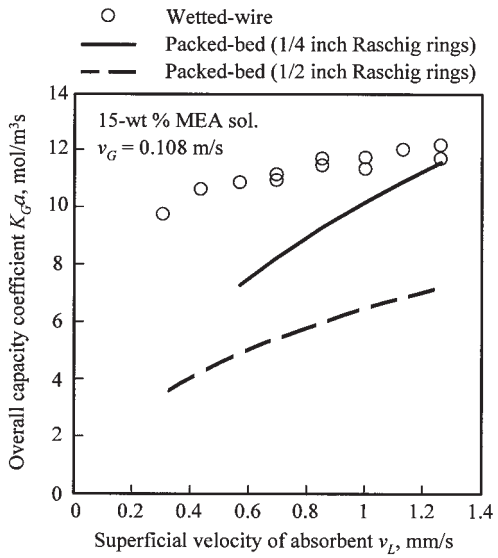

Figure 6. Comparison in gas-absorption performance between wetted-wire and packed-bed columns operated at the same gas–liquid supply conditions.

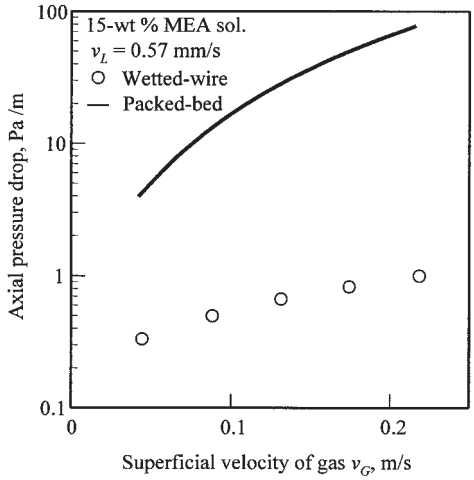

Figure 7. Comparison in axial gas-phase pressure drop between wetted-wire and packed-bed columns operated at the same gas–liquid supply conditions.

The packed-bed column is assumed to be packed with 1/2-in. Raschig rings.

Raschig rings, and the K_Ga values available by the column are predicted by a conventional procedure based on empirical correlations for gas–liquid flow and mass transfer in packed-bed columns, which is outlined in Appendix B. A set of K_Ga vs. v_L data obtained with the prototype wetted-wire column and corresponding predictions for the packed-bed column are plotted together in Figure 6. There we find that the wetted-wire column that we constructed possibly surpasses, in gas-absorption performance, the packed-bed column with 1/2- or 1/4-in. Raschig rings. Qualitatively speaking, the v_L dependency of K_Ga for the wetted-wire column is weaker than that for the packed-bed column, and thus the potential advantage of the wetted-wire column to the packed-bed column tends to extend with a decrease in v_L.

Concerning the issue of power consumption for gas–liquid contact operations, the wetted-wire column seems to be far superior to the packed-bed column. Figure 7 compares the gas-stream pressure drop measured with the wetted-wire column to that estimated for the packed-bed column with 1/2-in. Raschig rings. As outlined in Appendix C, the estimation for the packed-bed column is based on the empirical correlation advanced by Leva.[17] Although no quantitative estimation for the packed-bed column with 1/4-in. Raschig rings is possible because of the lack of relevant data, we can reasonably presume that the pressure drop for the case of using 1/4-in. Raschig rings is more or less larger than that for the case of using 1/2-in. Raschig rings under the same gas–liquid supply conditions. In Figure 7, we can readily recognize that the pressure drop in the wetted-wire column is lower than that in the packed-bed column by one to two orders of magnitude. This fact is not surprising, considering the void fraction in the wetted-wire column is as high as 0.98 (to be compared with that in the packed-bed column, 0.62–0.64; see Table B1) as well as the shape of the on-wire flow of the liquid absorbent that should cause little form drag to the gas flow.

Conclusions

A prototype of *wetted-wire columns*, novel gas–liquid contactors conceptually presented in our previous studies,[1,2] was first constructed to test its performance as a device for gas absorption. The prototype column equipped with 0.88-mm-diameter wires in staggered alignment at 6-mm intervals was found to show a gas-absorption performance (as evaluated in terms of the gas-based overall capacity coefficient) higher than that of conventional packed-bed columns with 1/2- or 1/4-in. Raschig rings, while causing the gas stream through it to show only a pressure drop not larger than one tenth of values that the packed-bed columns would show. This fact demonstrates the potential advantage of *wetted-wire columns* over conventional types of contactors, such as packed-bed columns, for use in gas-absorption operations in which both high absorption efficiency and low energy consumption for sustaining the operations are required.

Acknowledgments

This study was supported by a Grant-in-Aid for Scientific Research from the Japan Society for the Promotion of Science (Grant No. 13450087). We thank Suguru Okano, student in the Department of Mechanical Engineering, Keio University, for help in revising the manuscript.

Literature Cited

1. Chinju H, Uchiyama K, Mori YH. "String-of-beads" flow of liquids on vertical wires for gas absorption. *AIChE J*. 2000;46:937-945.
2. Uchiyama K, Migita H, Ohmura R, Mori YH. Gas absorption into "string-of-beads" liquid flow with chemical reaction: Application to carbon dioxide separation. *Int J Heat Mass Transfer*. 2003;46:457-468.
3. Song J-H, Park S-B, Yoon J-H, Lee H. Densities and viscosities of monoethanolamine + ethylene glycol + water. *J Chem Eng Data*. 1996;41:1152-1154.
4. Reid RC, Prausnitz JM, Sherwood TK. *The Properties of Gases and Liquids*. 3rd Edition. New York, NY: McGraw-Hill; 1977.
5. Hikita H, Ishikawa H, Uku K, Murakami T. Diffusivities of mono-, di-, and triethanolamines in aqueous solutions. *J Chem Eng Data*. 1980; 25:324-325.
6. Vázquez G, Alvarez E, Navaza JM, Rendo R, Romero E. Surface tension of binary mixtures of water + monoethanolamine and water + 2-amino-2-methyl-1-propanol and tertiary mixtures of these amines with water from 25°C to 50°C. *J Chem Eng Data*. 1997;42:57-59.
7. Lee JI, Otto FD, Mather AE. Equilibrium between carbon dioxide and aqueous monoethanolamine solutions. *J Appl Chem Biotechnol*. 1976; 26:541-549.
8. Muhlbauer HG, Monaghan PR. Sweetening natural gas with ethanolamine solutions. *Oil Gas J*. 1957;28:139-145.
9. Jou F-Y, Mather AE, Otto FD. The solubility of CO_2 in a 30 mass percent monoethanolamine solution. *Can J Chem Eng*. 1995;73:140-147.
10. Laddha SS, Danckwerts PV. Reaction of CO_2 with ethanolamines: Kinetics from gas-absorption. *Chem Eng Sci*. 1981;36:479-482.
11. Versteeg GF, Swaaij WPM. Solubility and diffusivity of acid gases (CO_2, N_2O) in aqueous alkanolamine solutions. *J Chem Eng Data*. 1988;33:29-34.
12. Joosten GEH, Danckwerts PV. Solubility and diffusivity of nitrous oxide in equimolar potassium carbonate–potassium bicarbonate solutions at 25°C and 1 atm. *J Chem Eng Data*. 1972;17:452-455.
13. Sada E, Kumazawa H, Butt MA. Solubility and diffusivity of gases in aqueous solutions of amines. *J Chem Eng Data*. 1978;23:161-163.
14. Wilke CR, Chang P. Correlation of diffusion coefficients in dilute solutions. *AIChE J*. 1955;1:264-270.
15. Hayduk W, Laudie H. Prediction of diffusion coefficients for nonelectrolytes in dilute aqueous solutions. *AIChE J*. 1974;20:611-615.
16. Hikita H, Asai S, Katsu Y, Ikuno S. Absorption of carbon dioxide into aqueous monoethanolamine solutions. *AIChE J*. 1979;25:793-800.
17. Leva M. Flow through irrigated dumped packings: Pressure drop, loading, flooding. *Chem Eng Prog Symp Ser*. 1954;50:51-59.
18. Ikame M, Kan S, Hiraoka K, Kumakura T. CO_2 absorption characteristics of packed column using aqueous solution of monoethanolamine (in Japanese). *Papers Ship Res Inst*. 1994;31:159-173.
19. Onda K, Takeuchi H, Koyama Y. Effect of packing materials on the wetted surface area (in Japanese). *Kagaku Kogaku*. 1967;31:126-134.
20. Onda K, Takeuchi H, Okumoto Y. Mass transfer coefficients between gas and liquid phases in packed columns. *J Chem Eng Jpn*. 1968;1: 56-62.
21. Onda K, Sada E, Takeuchi H. Gas absorption with chemical reaction in packed columns. *J Chem Eng Jpn*. 1968;1:62-66.
22. Perry RH, Green DW, Maloney JO, eds. *Perry's Chemical Engineers' Handbook*. 6th Edition. New York, NY: McGraw-Hill; 1984.
23. Society of Chemical Engineers, Japan, ed. *Kagaku Kogaku Binran*. 6th Edition. Tokyo: Maruzen; 1999.

Appendix A: Expression for Gas-Based Overall Capacity Coefficient

Assuming a steady, unidirectional plug flow of a CO_2/N_2 gas mixture inside the test column, we can write the conservation of CO_2 in the differential control volume illustrated in Figure A1 as

$$d(\tilde{m}_G y) = \tilde{m}_n dY = K_G(y - y^*)a\,dz \qquad \text{(A1)}$$

where $\tilde{m}$ is the superficial molar flux of the CO_2/N_2 gas mixture upwardly passing through the control volume, y is the mixed-mean mole fraction of CO_2 in the gas mixture, y^* is the CO_2 mole fraction in the gas mixture that would be in equilibrium with the mixed-mean mole fraction of CO_2 physically dissolved in the MEA solution, a is the gas–liquid interfacial area per unit volume, and z is the vertical distance measured downward from the top end of the gas–liquid contact section of the column. Note that $\tilde{m}_n$ is an invariant and thus handles more easily than $\tilde{m}_G$ in the following procedure. By integrating Eq.

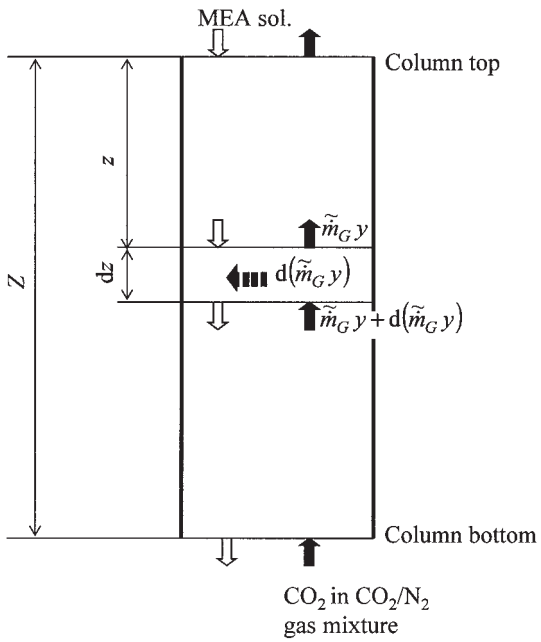

Figure A1. One-dimensional mass-balance model for the gas–liquid contact section in a gas-absorption column.

1 from the top ($z = 0$) to the bottom ($z = Z$) of the gas–liquid contact section, we obtain

$$Z = \frac{\tilde{m}_n}{K_G a} \int_{y_T}^{y_B} \frac{dY}{y - y^*} \tag{A2}$$

Considering that y^* is negligibly small compared to unity in the range of the present experiments, Eq. A2 may be modified as follows

$$Z = \frac{\tilde{m}_n}{K_G a} \int_{y_T}^{y_B} \frac{dY}{y} = \frac{\tilde{m}_n}{K_G a} \int_{Y_T}^{Y_B} \left(1 + \frac{1}{Y}\right) dY = \frac{\tilde{m}_n}{K_G a} \left[Y_B - Y_T + \ln\left(\frac{Y_B}{Y_T}\right) \right] \tag{A3}$$

From this equation we can readily obtain Eq. 2, an expression for the capacity coefficient $K_G a$. The above formulation generally follows the one that Ikame et al.[18] described in their research report on CO_2 absorption in a packed-bed column.

Appendix B: Calculating Capacity Coefficient for a Packed-Bed Column

The molar flux of CO_2 at the gas–liquid interface in a packed-bed column, $\tilde{m}_i$, may be expressed in some alternative ways, such as

$$\tilde{m}_i = k'_G(p - p_i) = k_G \tilde{\rho}_G (y - y_i) = \beta k_L \tilde{\rho}_L (x_i - x) = K_G (y - y^*) \tag{B1}$$

where p and y are the mixed-mean partial pressure and mole fraction, respectively, of CO_2 in the gas mixture at a given z position; p_i and y_i are the partial pressure and mole fraction, respectively, of CO_2 on the gas side at the gas–liquid interface; x_i is the mole fraction of CO_2 on the liquid side at the interface; x is the mixed-mean mole fraction of CO_2 physically dissolved in the liquid absorbent; y^* is the CO_2 mole fraction in the gas mixture that would be equilibrated with the liquid absorbent in which CO_2 is physically dissolved to x; $\tilde{\rho}_G$ and $\tilde{\rho}_L$ are molar densities of the gas mixture and the liquid absorbent, respectively; and β is a nondimensional reaction factor representing the promotion effect of the CO_2–MEA reaction on the mass transfer of CO_2. Note that among the four *mass transfer coefficients* defined in Eq. B1, only the gas-side mass transfer coefficient k_G and the liquid-side mass transfer coefficient k_L have the standard dimension expressed as m/s according to the SI; k'_G and K_G have different dimensions expressed by the units of mol m^{-2} s^{-1} Pa^{-1} and mol m^{-2} s^{-1}, respectively. Introducing Henry's constant H (defined as the ratio of CO_2 molar concentration in a liquid phase to CO_2 vapor pressure in a gas phase in mutual equilibrium) and the total pressure of the gas mixture (that is, the system pressure) P, we can rewrite Eq. B1 as

$$\tilde{m}_i = k'_G P\left(\frac{p}{P} - \frac{p_i}{P}\right) = k_G \tilde{\rho}_G (y - y_i) = \beta k_L H P \left(\frac{p_i}{P} - \frac{p^*}{P}\right) = K_G (y - y^*) \tag{B2}$$

where p^* denotes the pressure of CO_2 in the gas mixture that would be in equilibrium with the liquid absorbent in which CO_2 is physically dissolved to the mole fraction of x. If we assume the CO_2/N_2 mixture to be an ideal-gas mixture, we can further rewrite the above equation as follows

$$\tilde{m}_i = k'_G P (y - y_i) = k_G \tilde{\rho}_G (y - y_i) = \beta k_L H P (y_i - y^*) = K_G (y - y^*) \tag{B3}$$

From Eq. B3 we can relate K_G to k_G or k'_G and k_L as

$$\frac{1}{K_G} = \frac{1}{k_G \tilde{\rho}_G} + \frac{1}{\beta k_L H P} = \frac{1}{P}\left(\frac{1}{k'_G} + \frac{1}{\beta k_L H}\right) \tag{B4}$$

To evaluate the overall capacity coefficient $K_G a$, we need to combine appropriate correlations for a, k_G or k'_G, k_L, and β with Eq. B4. The following correlations for a, k'_G, and k_L were prepared by Onda et al.[19,20]

$$\frac{a}{a_t} = 1 - \exp\left[-1.45 \left(\frac{\sigma_c}{\sigma}\right)^{0.75} \left(\frac{\dot{m}_L}{a_t \mu_L}\right)^{0.1} \left(\frac{\dot{m}_L^2 a_t}{\rho_L^2 g}\right)^{-0.05} \left(\frac{\dot{m}_L^2}{\rho_L \sigma a_t}\right)^{0.2} \right] \tag{B5}$$

$$\frac{k'_G \tilde{R} T}{a_t D_G} = 2.0 \left(\frac{\dot{m}_G}{a_t \mu_G}\right)^{0.7} \left(\frac{\mu_G}{\rho_G D_G}\right)^{1/3} (a_t d_p)^{-2.0} \qquad (d_p < 15 \text{ mm}) \tag{B6}$$

$$k_L \left(\frac{\rho_L}{\mu_L g}\right)^{1/3} = 0.0051 \left(\frac{\dot{m}_L}{a \mu_L}\right)^{2/3} \left(\frac{\mu_L}{\rho_L D_L}\right)^{-1/2} (a_t d_p)^{0.4} \tag{B7}$$

where a_t is the total surface area of the packings per unit volume of the packed bed; σ_c is the critical surface tension of the packing material; σ is the surface tension of the liquid absorbent; $\dot{m}_L$ and $\dot{m}_G$ are the superficial mass fluxes of the absorbent and the gas mixture, respectively, across a horizontal cross section of the test column; ρ_L and ρ_G are the mass densities of the absorbent and the gas mixture; μ_L and μ_G are the viscosities of the absorbent and the gas mixture; g is the acceleration arising from gravity; $\tilde{R}$ is the universal gas constant; T is the system temperature; D_L and D_G are the mass diffusivity of CO_2 in the absorbent and that in the gas mixture, respectively; and d_p is the nominal size of the packings. Although Eqs. B5–B7 are widely cited in the literature as they are, they may be rewritten to be more consistent with the general style of formulating fluid-mechanical and mass-transfer phenomena as

$$\frac{a}{a_t} = 1 - \exp\left[-1.45 \left(\frac{\sigma_c}{\sigma}\right)^{0.75} \left(\frac{v_L}{a_t \nu_L}\right)^{0.1} \left(\frac{v_L^2 a_t}{g}\right)^{-0.05} \left(\frac{\rho_L v_L^2}{\sigma a_t}\right)^{0.2} \right] \tag{B8}$$

$$\frac{k_G}{a_t D_G} = 2.0\left(\frac{\nu_G}{a_t \nu_G}\right)^{0.7}\left(\frac{\nu_G}{D_G}\right)^{1/3}(a_t d_p)^{-2.0} \qquad (d_p < 15 \text{ mm}) \tag{B9}$$

$$\frac{k_L}{a_t D_L} = 0.0051\left(\frac{\nu_L}{a\nu_L}\right)^{2/3}\left(\frac{\nu_L}{D_L}\right)^{1/2}\left(\frac{g}{a_t^3 \nu_L^2}\right)^{1/3}(a_t d_p)^{0.4} \tag{B10}$$

where ν_G and ν_L are the kinematic viscosities of the gas mixture and liquid absorbent, respectively. Assuming a_t^{-1} and a^{-1} as the representative lengths for the gas and liquid flows, respectively, we can view Eqs. B9 and B10 as expressions for gas- and liquid-side Sherwood numbers, respectively, each correlated to a relevant Reynolds number, a Schmidt number, a packing geometrical factor ($a_t d_p$) and, in Eq. B10, a Galileo number.

The value of β is determined by an iterative calculation using the van Krevelen–Hoftijzer equation, which may be written as[21]

$$\beta = \frac{\gamma\left(1 - \dfrac{\beta - 1}{rq}\right)^{1/2}}{\tanh\left[\gamma\left(1 - \dfrac{\beta - 1}{rq}\right)^{1/2}\right]} \tag{B11}$$

where $\gamma = (k_r \tilde{C}_{\text{mean}} D_L)^{1/2}/k_L$; k_r is the CO_2–MEA reaction rate constant; $\tilde{C}_{\text{mean}}$is the arithmetic mean of $\tilde{C}_T$ and $\tilde{C}_B$, the mixed-mean molar concentrations of MEA in the liquid absorbent at the top and the bottom, respectively, of the packed-bed column; r is the ratio of D_{AL}, the diffusivity of MEA in the absorbent, to D_L; $q = \tilde{C}_{\text{mean}}/(\nu \tilde{c}_s)$; $\tilde{c}_s$ is the physical solubility of CO_2 in the absorbent; ν is the MEA-to-CO_2 stoichiometric ratio (=2). $\tilde{C}_{\text{mean}}$needs to be determined iteratively by the following procedure:

(1) Substitute the value of $\tilde{C}_T$ (that is, the molar MEA concentration in the absorbent to be supplied to the packed-bed column) into $\tilde{C}_{\text{mean}}$ and calculate $K_G a$, using Eqs. B4 and B8–B11.

(2) Substitute the value of $K_G a$ thus obtained into Eq. 2 to determine $\tilde{m}_n(Y_B - Y_T)$.

(3) Calculate the corresponding reduction in MEA concentration in the absorbent from $\tilde{C}_T$ to $\tilde{C}_B$, assuming that all CO_2 molecules absorbed into the absorbent are reacted with MEA at the stoichiometric ratio ($\nu = 2$).

(4) Calculate $(\tilde{C}_T + \tilde{C}_B)/2$, substitute it into $\tilde{C}_{\text{mean}}$, and repeat the calculations of $K_G a$, $\tilde{m}_n(Y_B - Y_T)$, $(\tilde{C}_T - \tilde{C}_B)$, and $(\tilde{C}_T + \tilde{C}_B)/2 = \tilde{C}_{\text{mean}}$, until $\tilde{C}_{\text{mean}}$ thus deduced no longer changes through further repetitive calculations.

Table B1 gives the values of a_t and σ_c for use in predicting $K_G a$ for a virtual packed-bed column, which is to be compared with the wetted-wire column we experimentally tested in the present study.

Table B1. Specifications for a Packed-Bed Column Assumed to be Operated at a Temperature of 25°C and a Pressure of 101.3 kPa

Packing type	Raschig ring	
Packing material	Ceramic	
Critical surface tension of packing material, σ_c (mN/m)	61*	
Nominal packing size, d_p	1/2 in. (12.7 mm)	1/4 in. (6.4 mm)
Specific packing surface area, a_t (m^2/m^3)	370**	710**
Void fraction	0.64**	0.62**
Coefficient α in Eq. C1	1700†	
Coefficient β in Eq. C1	83.9†	

*Estimated from experimental data obtained by Onda et al.[20]
**Cited from Table 18-5 in *Perry's Chemical Engineers' Handbook.*[22]
†Cited from Table 11.5 in *Kagaku Kogaku Binran.*[23]

Appendix C: Estimating Pressure Drop in Gas Stream in a Packed-Bed Column

The axial gas-stream pressure drop in a packed-bed column may be estimated by use of Leva's correlation.[17] This correlation is dimensionally inconsistent, and the use of U.S. customary units is required in its original form. The following is its SI-based expression:

$$\frac{\Delta p/Z}{[\text{Pa m}^{-1}]} = -\alpha(10^{\beta \nu_L/[\text{m s}^{-1}]})\left(\frac{\rho_G \nu_G^2}{[\text{Pa}]}\right) \tag{C1}$$

where Δp is the pressure drop over the axial length Z. The coefficients α and β were given by Leva[17] for Raschig rings of 3/4 in. in nominal size or larger. Later the coefficients for 1/2-in. Raschig rings were added[22,23] but not yet for even smaller rings. The coefficients for 1/2-in. Raschig rings to be consistent with Eq. C1 are given in Table B1.

Manuscript received Apr. 21, 2004, and revision received Dec. 10, 2004.